

## Synthesis and Characterisation of Ruthenium Complexes Containing a Pendent Catechol Ring

Luke O'Brien,<sup>a</sup> Marco Duati,<sup>a</sup> Sven Rau,<sup>b</sup> Adrian L. Guckian,<sup>a</sup> Tia E. Keyes,<sup>a</sup> Noel M. O'Boyle,<sup>a</sup> Andreas Serr,<sup>ac</sup> Helmar Görls<sup>b</sup> and Johannes G. Vos<sup>\*a</sup>

<sup>a</sup> National Centre for Sensor Research, School of Chemical Sciences, Dublin City University, Dublin 9, Ireland. Fax: +353 1 7005503; Tel: +353 1 7005307; E-mail: johannes.vos@dcu.ie

<sup>b</sup> Institut für Anorganische und Analytische Chemie, Friedrich-Schiller-University, 07743, Jena, Germany. Fax: +49 3641 948102; Tel: +49 3641 948113; E-mail: Sven.Rau@uni-jena.de

<sup>c</sup> Fakultät für Chemie, Universität Bielefeld, D-33615 Bielefeld, Germany. E-mail: Andreas.Serr@uni-bielefeld.de

**This submission was created using the RSC Article Template (DO NOT DELETE THIS TEXT)  
(LINE INCLUDED FOR SPACING ONLY - DO NOT DELETE THIS TEXT)**

A series of  $[\text{Ru}(\text{bipy})_2\text{L}]^+$  and  $[\text{Ru}(\text{phen})_2\text{L}]^+$  complexes where L is 2-[5-(3,4-dimethoxyphenyl)-4H-1,2,4-triazol-3-yl]pyridine (**HL1**) and 4-(5-pyridin-2-yl-4H-1,2,4-triazol-3-yl)benzene-1,2-diol (**HL2**) are reported. The compounds obtained have been characterised using x-ray crystallography, NMR, UV/Vis and emission spectroscopies. Partial deuteration is used to determine the nature of the emitting state and to simplify the NMR spectra. The acid-base properties of the compounds are also investigated. The electronic structure of the **HL1** complex is examined using ZINDO. Electro and spectroelectrochemical studies on  $[\text{Ru}(\text{bipy})_2(\text{L2})]^+$  suggest that proton transfer between the catechol and triazole moieties on **L2** takes place upon oxidation of the **L2** ligand.

### Introduction

The hydroquinone/quinone redox couple plays an essential role as electron mediator in the charge separation processes in photosynthesis.<sup>1</sup> As a result there has been extensive interest in the redox properties of quinone containing metal complexes and in their potential to act as electron acceptors or donors.<sup>2</sup> In these studies catechol based ligands are coordinated to a wide range of metals.<sup>3</sup> Much less attention has been paid to the interaction between metal centres and pendent hydroquinone/quinone groupings, although such materials may participate in light induced electron transfer reactions.<sup>4</sup> We are presently involved in a systematic study of the electrochemical and photophysical properties of ruthenium complexes containing pendent hydroquinone/quinones.<sup>5,6</sup> In an earlier study on ruthenium polypyridyl complexes incorporating pyridyltriazole ligands with free hydroquinone groupings, electrochemically induced intramolecular protonation of the ruthenium centre was observed upon oxidation of the hydroquinone moiety.<sup>6</sup> In this contribution the synthesis and deprotection of the methoxy complexes  $[\text{Ru}(\text{bipy})_2(\text{L1})]\text{PF}_6 \cdot 5\text{H}_2\text{O}$  and  $[\text{Ru}(\text{phen})_2(\text{L1})]\text{PF}_6 \cdot 2\text{H}_2\text{O}$  (where **HL1** is 2-[5-(3,4-dimethoxyphenyl)-4H-1,2,4-triazol-3-yl]pyridine) to produce the catechol type complexes with the ligand **HL2** 4-(5-Pyridin-2-yl-4H-1,2,4-triazol-3-yl)benzene-1,2-diol are described (for ligand structures see Figure 1). The partially deuterated analogues  $[\text{Ru}(d_8\text{-bipy})_2(\text{L1})]^+$  and  $[\text{Ru}(d_8\text{-phen})_2(\text{L1})]^+$  are also described. The materials obtained have been characterised by X-ray crystallography and <sup>1</sup>H-NMR spectroscopy. The absorption, emission, photophysical and electrochemical properties of the complexes are also examined. To aid interpretation of the results obtained, semi-empirical calculations using ZINDO were carried out on  $[\text{Ru}(\text{bipy})_2(\text{HL1})]^{2+}$  and  $[\text{Ru}(\text{bipy})_2(\text{L1})]^+$ , where the triazole moieties are in the protonated and deprotonated states respectively.

### Experimental

All synthetic reagents were of commercial grade and used without further purification. The solvents used in spectroscopic measurements were HPLC grade. Perdeuterated 1,10-phenanthroline (*d*<sub>8</sub>-phen) and perdeuterated 2,2'-bipyridyl (*d*<sub>8</sub>-bipy) were obtained using established methods.<sup>7</sup> *cis*- $[\text{Ru}(\text{bipy})_2\text{Cl}_2] \cdot 2\text{H}_2\text{O}$ , *cis*- $[\text{Ru}(d_8\text{-bipy})_2\text{Cl}_2] \cdot 2\text{H}_2\text{O}$ , *cis*- $[\text{Ru}(\text{phen})_2\text{Cl}_2] \cdot 2\text{H}_2\text{O}$  and *cis*- $[\text{Ru}(d_8\text{-phen})_2\text{Cl}_2]$  were synthesised using literature methods.<sup>8</sup>

#### 2-[5-(3,4-dimethoxyphenyl)-4H-1,2,4-triazol-3-yl]pyridine

**(HL1)**. A solution of 2-picolylamhydrazone 0.01 mol (1.36g) and 0.015 mol (1.5g) triethylamine in 30 cm<sup>3</sup> of dry THF was vigorously stirred and cooled to 0°C with an ice bath. 3,4-dimethoxy-benzoylchloride 0.01 mol (2.005g) in 10 cm<sup>3</sup> THF was added dropwise to this solution and the reaction mixture was heated at reflux for a further 5 min. The volume was reduced to half *in vacuo*. An equal amount of water was added and the flask stored overnight at 4°C. The white precipitate was collected by filtration, washed with water and dried under vacuum. The solid obtained was recrystallised from ethylene glycol:water to yield 1.7 g (70%). <sup>1</sup>H NMR in *d*<sub>6</sub>-dmsO 8.73 (1H,d,H<sup>6</sup>), 8.19 (1H,d,H<sup>3</sup>), 8.01 (1H,dd,H<sup>4</sup>), 7.68 (1H,s,H<sup>2</sup>), 7.66 (1H,d,H<sup>6</sup>), 7.52 (1H,dd,H<sup>5</sup>), 7.11 (1H,d,H<sup>5</sup>), 3.87 (3H,s,OMe), 3.83 (3H,s,OMe), mp = 186-188°C.

$[\text{Ru}(\text{bipy})_2(\text{L1})]\text{PF}_6 \cdot \text{H}_2\text{O}$  0.395 g (1.41 mmol) of **HL1** was dissolved in 50 cm<sup>3</sup> ethanol:water (1:1 v/v) and the mixture was heated at reflux until the ligand was fully dissolved. 0.520g (1 mmol) *cis*- $[\text{Ru}(\text{bipy})_2\text{Cl}_2] \cdot 2\text{H}_2\text{O}$  was added and the reaction allowed to reflux for 8 hours. The reaction was monitored by analytical HPLC. After cooling the reaction mixture was filtered and the volume reduced to *circa* 15 cm<sup>3</sup>. The complex was precipitated by addition of a concentrated aqueous solution of ammonium hexafluorophosphate. The precipitate was filtered and washed with water. The crude complex was recrystallised from acetone/water (2:1 v/v) to which a few drops of aqueous NH<sub>3</sub> were added. The complex was further purified by column chromatography on neutral alumina using acetonitrile as eluent and recrystallised as outlined above. <sup>1</sup>H-NMR in *d*<sub>3</sub>-acetonitrile for coordinated L1; 8.08(1H,d,H<sup>3</sup>); 7.89(1H,dd,H<sup>4</sup>); 7.10(1H,dd,H<sup>5</sup>); 7.46(1H,d,H<sup>6</sup>); 7.49(1H,s,H<sup>2</sup>); 7.48(1H,d,H<sup>6</sup>) 6.88(1H,d,H<sup>5</sup>). Yield = 0.53 g (60 %). Calcd. for :  $\text{RuC}_{35}\text{H}_{31}\text{N}_8\text{O}_3\text{PF}_6$  C: 49.00; H: 3.60; N: 13.10 %. Anal. Found: C: 48.58; H: 3.34; N: 12.66 %.

$[\text{Ru}(\text{phen})_2(\text{L1})]\text{PF}_6 \cdot \text{H}_2\text{O}$  was prepared and purified as described for  $[\text{Ru}(\text{bipy})_2(\text{L1})]\text{PF}_6 \cdot \text{H}_2\text{O}$ . <sup>1</sup>H NMR in *d*<sub>3</sub>-acetonitrile for coordinated L1; 8.14(1H,d,H<sup>3</sup>); 7.87(1H,dd,H<sup>4</sup>); 7.01(1H,dd,H<sup>5</sup>); 7.49(1H,d,H<sup>6</sup>); 7.47(1H,s,H<sup>2</sup>); 7.40(1H,d,H<sup>6</sup>) 6.86(1H,d,H<sup>5</sup>). Yield = 0.45 g (50%). Calcd. for :  $\text{RuC}_{39}\text{H}_{31}\text{N}_8\text{O}_3\text{PF}_6$  C: 51.72; H: 3.45; N: 12.37 %. Anal. Found: C: 52.12; H: 3.54; N: 12.17 %.

$[\text{Ru}(d_8\text{-bipy})_2(\text{L1})]\text{PF}_6 \cdot \text{H}_2\text{O}$  was prepared and purified as reported for  $[\text{Ru}(\text{bipy})_2(\text{L1})]\text{PF}_6 \cdot \text{H}_2\text{O}$ . <sup>1</sup>H NMR in *d*<sub>3</sub>-acetonitrile for coordinated L1; 8.13(1H,d,H<sup>3</sup>); 7.88(1H,dd,H<sup>4</sup>);

7.14(1H,dd,H<sup>5</sup>); 7.47(1H,d,H<sup>6</sup>); 7.52(1H,s,H<sup>2</sup>); 7.49(1H,d,H<sup>6</sup>); 6.90(1H,d,H<sup>5</sup>). Yield = 0.46 g (54 %). Calcd. for : RuC<sub>35</sub>H<sub>15</sub>D<sub>16</sub>N<sub>8</sub>O<sub>3</sub>PF<sub>6</sub> C: 48.11; H: 3.55; N: 12.82 %. Anal. Found: C: 47.90; H: 3.48; N: 12.49 %.

[Ru(*d*<sub>8</sub>-phen)<sub>2</sub>(L1)]PF<sub>6</sub>·H<sub>2</sub>O was prepared and purified as described for [Ru(bipy)<sub>2</sub>(L1)]PF<sub>6</sub>·H<sub>2</sub>O. <sup>1</sup>H NMR in d<sub>3</sub>-acetonitrile for coordinated L1; 8.12(1H,d,H<sup>3</sup>); 7.84(1H,dd,H<sup>4</sup>); 6.99(1H,dd,H<sup>5</sup>); 7.45(1H,d,H<sup>6</sup>); 7.42(1H,s,H<sup>2</sup>); 7.39(1H,d,H<sup>6</sup>); 6.83(1H,d,H<sup>5</sup>). Yield = 0.52 g (56 %). Calcd. for : RuC<sub>39</sub>H<sub>15</sub>D<sub>16</sub>N<sub>8</sub>O<sub>3</sub>PF<sub>6</sub> C: 50.80; H: 3.39; N: 12.16 %. Anal. Found: C: 50.75; H: 3.42; N: 11.91 %.

[Ru(bipy)<sub>2</sub>(L2)]PF<sub>6</sub>·5H<sub>2</sub>O was prepared by demethylation of [Ru(bipy)<sub>2</sub>(L1)]<sup>+</sup> with boron tribromide.<sup>9</sup> 0.523 g (0.61 mmol) of [Ru(bipy)<sub>2</sub>(L1)]PF<sub>6</sub>·H<sub>2</sub>O was dissolved and stirred in 20 cm<sup>3</sup> dry dichloromethane under N<sub>2</sub>. The flask was placed in a toluene/liquid nitrogen bath (-78 °C) and allowed to equilibrate for at least 20 min. 12 cm<sup>3</sup> (ten fold molar excess) of 1.0 M boron tribromide in dichloromethane was slowly added to the reaction flask. The reaction was left stirring at -78 °C for at least one hour under N<sub>2</sub> and allowed warm to room temperature overnight. The reaction was quenched by slow addition of iced water to the reaction flask. The reaction mixture was neutralised by adding an aqueous solution of concentrated sodium carbonate. The deep red product was precipitated using saturated aqueous NH<sub>4</sub>PF<sub>6</sub>. The product was washed with diethyl ether and recrystallised from acetone/water (2:1). <sup>1</sup>H NMR resonances of coordinated L2 in d<sub>3</sub>-acetonitrile 8.25(1H,d,H<sup>3</sup>); 7.96(1H,dd,H<sup>4</sup>); 7.28 (1H,dd,H<sup>5</sup>); 7.54 (1H,d,H<sup>6</sup>); 7.34 (1H,s,H<sup>3</sup>); 7.26 (1H,d,H<sup>5</sup>); 6.84(1H,d,H<sup>6</sup>). Yield = 0.351 g (64 %). Calcd. for : RuC<sub>33</sub>H<sub>35</sub>N<sub>8</sub>O<sub>7</sub>PF<sub>6</sub> C: 43.96; H: 3.91; N: 12.42 %. Anal. Found: C: 43.83; H: 4.00; N: 12.24 %.

[Ru(phen)<sub>2</sub>(L2)]PF<sub>6</sub>·2H<sub>2</sub>O [Ru(phen)<sub>2</sub>(L1)]<sup>+</sup> was deprotected to form [Ru(phen)<sub>2</sub>(L2)]PF<sub>6</sub>·2H<sub>2</sub>O using BBr<sub>3</sub> in a similar reaction to that described for [Ru(bipy)<sub>2</sub>(L2)]PF<sub>6</sub>·5H<sub>2</sub>O. <sup>1</sup>H-NMR resonances of L2 in d<sub>3</sub>-acetonitrile 8.19(1H,d, H<sup>3</sup>); 7.87(1H,dd,H<sup>4</sup>); 7.01 (1H,dd,H<sup>5</sup>); 7.42 (1H,d,H<sup>6</sup>); 7.30 (1H,s,H<sup>3</sup>); 7.18 (1H,d,H<sup>5</sup>); 6.85(1H,d,H<sup>6</sup>). Yield = 0.535 g (83 %). Calcd. for : RuC<sub>37</sub>H<sub>29</sub>N<sub>8</sub>O<sub>4</sub>PF<sub>6</sub> C: 49.62; H: 3.26; N: 12.51 %. Anal. Found: C: 49.86; H: 3.26; N: 12.17 %.

## Instrumental methods

<sup>1</sup>H and <sup>1</sup>H COSY spectra were recorded on a Bruker AC400 (400 MHz) instrument. Peak positions are relative to residual solvent peaks. UV/Visible spectra were obtained using a Shimadzu UV3100 UV-Vis-NIR spectrophotometer interfaced to an Elonex PC433 personal computer. Extinction coefficients are accurate to 5 %. Emission spectra were obtained on a Perkin-Elmer LS50-B luminescence spectrometer equipped with a red sensitive Hamamatsu R928 detector, interfaced to an Elonex PC466 personal computer employing Perkin-Elmer FL WinLab custom built software. Excitation and emission slit widths of 10 nm were used. The spectra were not corrected for photomultiplier response. HPLC grade acetonitrile was used as a solvent. To ensure protonation/deprotonation, 50 μL perchloric acid or diethyl amine solution were added to the sample. pK<sub>a</sub> values were determined in Britton-Robinson buffer (0.04 M boric acid, 0.04 M acetic acid, 0.04 M phosphoric acid). The pH was adjusted by adding conc. NaOH or conc. H<sub>2</sub>SO<sub>4</sub> and was measured using a Corning 240 digital pH meter. The pK<sub>a</sub> values were determined from the point of inflection of the absorbance versus pH plot. Excited state acid-base equilibria were measured from the changes in the emission intensity as a function of pH (*vide infra*). A suitable isosbestic point in the absorption titration curves was taken as excitation wavelength. Luminescence lifetime measurements were obtained using an Edinburgh Analytical Instruments (EAI) Time-Correlated

Single-Photon Counting apparatus (TCSPC). Samples were deaerated for 20 min using Ar gas before measurements were carried out, followed by repeated deaeration to ensure total oxygen exclusion. Emission lifetimes were calculated using a single exponential fitting function; Levenberg-Marquardt algorithm with iterative reconvolution (Edinburgh instruments F900 software) and are ± 10%. The χ<sup>2</sup> and residual plots were used to judge the quality of the fits. Measurements were performed in spectroscopic grade acetonitrile. The protonation state of the triazole rings was controlled as outlined above. Cyclic voltammetry and square wave voltammetry were carried out using a CHInstrument Model 660 potentiostat electrochemical workstation interfaced to an Elonex 486 PC. 0.1 M tetraethylammonium perchlorate (TEAP) in acetonitrile was used as electrolyte. A Ag/AgCl reference electrode, a 3 mm diameter teflon shrouded glassy carbon working electrode and a platinum gauze counter electrode were employed. TFA was added to ensure protonation of the complexes when needed) Samples were N<sub>2</sub> purged prior to measurements. Spectroelectrochemistry was carried out using electrochemical equipment as outlined above with a home-made pyrex glass thin layer cell (1 mm), a platinum gauze working electrode, a *pseudo*-Ag/AgCl reference electrode and a platinum wire counter electrode. Spectra were recorded in 0.1 M TEAP in CH<sub>3</sub>CN with the a Shimadzu 3100 UV-Vis/NIR spectrometer interfaced to an Elonex PC433 computer.

HPLC experiments were carried out using a Waters HPLC system, consisting of a model 501 pump, a 20 μl injector loop, a Partisil SCX steel column and a 990 photodiode array detector. The mobile phase used was 0.08 M LiClO<sub>4</sub> in 80/20 acetonitrile/water, the flow rate 1.8 cm<sup>3</sup>/min. C,H,N elemental analyses were carried out by the Microanalytical laboratories at University College Dublin.

X-ray Crystallography. Intensity data were collected on a Nonius KappaCCD diffractometer, using graphite-monochromated Mo-K<sub>α</sub> radiation. Data were corrected for Lorentz and polarisation effects, but not for absorption.<sup>10</sup> The structures were solved by direct methods (SHELXS<sup>11</sup>) and refined by full-matrix least squares techniques against Fo<sup>2</sup> (SHELXL-97<sup>12</sup>). The hydrogen atoms of the structures were included at calculated positions with fixed thermal parameters. The PF<sub>6</sub><sup>-</sup> groups of [Ru(phen)<sub>2</sub>(L1)]<sup>+</sup> and [Ru(*d*<sub>8</sub>-bipy)<sub>2</sub>(L1)]<sup>+</sup> are disordered, but this disorder could be solved. All non-hydrogen atoms were refined anisotropically.<sup>12</sup> XP (SIEMENS Analytical X-ray Instruments, Inc.) was used for structure representations.

Crystal Data for [Ru(phen)<sub>2</sub>(L1)]<sup>+</sup>:<sup>13</sup> C<sub>39</sub>H<sub>29</sub>F<sub>6</sub>N<sub>8</sub>O<sub>2</sub>PRu, Mr = 887.74 gmol<sup>-1</sup>, red-brown prism, size 0.38 x 0.32 x 0.28 mm<sup>3</sup>, monoclinic, space group P2<sub>1</sub>/c, a = 11.6379(9), b = 19.473(2), c = 16.879(1) Å, β = 102.944(7)°, V = 3728.0(5) Å<sup>3</sup>, T = -90 °C, Z = 4, ρ<sub>calcd.</sub> = 1.582 gcm<sup>-3</sup>, μ (Mo-K<sub>α</sub>) = 5.42 cm<sup>-1</sup>, F(000) = 1792, 7896 reflections in h(-14/14), k(-24/0), l(0/21), measured in the range 2.43° ≤ θ ≤ 26.42°, completeness Θ<sub>max</sub> = 99.4 %, 7631 independent reflections, R<sub>int</sub> = 0.029, 4848 reflections with F<sub>o</sub> > 4σ(F<sub>o</sub>), 508 parameters, 0 restraints, R<sub>1,obs</sub> = 0.053, wR<sub>2,obs</sub> = 0.142, R<sub>1,all</sub> = 0.116, wR<sub>2,all</sub> = 0.155, GOOF = 0.997, largest difference peak and hole: 0.996 / -0.558 e Å<sup>-3</sup>. CCDC reference Number 213441

Crystal Data for [Ru(*d*<sub>8</sub>-bipy)<sub>2</sub>(L1)]<sup>+</sup>:<sup>13</sup> C<sub>35</sub>H<sub>13</sub>D<sub>16</sub>F<sub>6</sub>N<sub>8</sub>O<sub>2</sub>PRu \* H<sub>2</sub>O, Mr = 848.71 gmol<sup>-1</sup>, colourless prism, size 0.32 x 0.30 x 0.20 mm<sup>3</sup>, red-brown, space group P2<sub>1</sub>/n, a = 9.1165(9), b = 18.068(1), c = 21.424(1) Å, β = 96.599(6)°, V = 3505.5(4) Å<sup>3</sup>, T = -90 °C, Z = 4, ρ<sub>calcd.</sub> = 1.608 gcm<sup>-3</sup>, μ (Mo-K<sub>α</sub>) = 5.73 cm<sup>-1</sup>, F(000) = 1716, 7296 reflections in h(-11/11), k(-22/0), l(0/26), measured in the range 2.34° ≤ θ ≤ 26.31°, completeness Θ<sub>max</sub> = 99.8 %, 7106 independent reflections, R<sub>int</sub> = 0.026, 4811 reflections with F<sub>o</sub> > 4σ(F<sub>o</sub>), 482 parameters, 0 restraints, R<sub>1,obs</sub> = 0.054, wR<sub>2,obs</sub> = 0.153, R<sub>1,all</sub> = 0.102, wR<sub>2,all</sub> = 0.167, GOOF =

0.995, largest difference peak and hole: 1.216 / -0.691 e Å<sup>-3</sup>.  
CCDC Reference Number 213442.

Calculations. INDO/1 and INDO/S semi-empirical calculations used the ZINDO method and HyperChem<sup>14</sup> on an Intel Pentium IV 1.6 GHz PC. Geometry optimisations were performed using the ZINDO/1 method. The default parameters for ruthenium as suggested by Anderson *et al.*<sup>15</sup> were used, apart from a value for the resonance integral,  $\beta(4d)$ , of -20.0 eV as suggested by Gorelsky *et al.*<sup>16</sup> The overlap weighting factors  $\sigma$ - $\sigma$  and  $\pi$ - $\pi$  for ZINDO/1 calculations were both set at 1. Convergence was assumed at a gradient went below 5 cal mol<sup>-1</sup> Å<sup>-1</sup>. Molecular orbital calculations were performed with ZINDO/S using the Krogh-Jespersen bases for ruthenium.<sup>17</sup> However, the electronic energy of the isolated atom was adjusted to the standard value for ZINDO/1. Values of 0.0, 0.9, and 0.1 respectively, were used for the fractional contributions of the d<sup>n-2</sup>s<sup>2</sup>, d<sup>n-1</sup>s(p) and d<sup>n</sup> configurations to the core integrals.<sup>18</sup> The overlap weighting factors  $\sigma$ - $\sigma$  and  $\pi$ - $\pi$  for ZINDO/S calculations were set at 1.265 and 0.585 as suggested by Ridley and Zerner.<sup>19</sup> Density of states spectra were constructed from the calculated ZINDO/S molecular orbital energies by convolution with gaussians of unit height and FWHM of 0.5 eV.

## Results and Discussion

### Synthetic Procedures.

The synthesis of the complexes based on **HL1** follows well-established preparation methods. As has been observed with other pyridyltriazole complexes the ligand **HL1** deprotonates upon coordination to the metal centre to form **L1**<sup>+</sup> and the complexes are therefore obtained as monocations upon the addition of excess PF<sub>6</sub><sup>-</sup>. To ensure that deprotonated complexes are obtained the products were recrystallised in the presence of a few drops of aqueous ammonia. The method applied for the deprotection of the methoxy compounds is a modification of literature methods, however, longer reaction times were needed to ensure complete demethylation. Successful demethylation was verified by HPLC and <sup>1</sup>H-NMR (*vide infra*).

### X-ray crystallography.

A feature of many pyridyltriazole ligands is the possibility of coordination via *N2* and *N4* of the triazole (See Figure 2 for 1,2,4-triazole labelling scheme). In a study carried out by Ryan *et al.* it was found that for ligands with a substituent on the triazole 5-position coordination occurred via both *N4* and *N2* in a ratio of approximately 9:1,<sup>20</sup> while the ratio of isomers is 1:1 when the 5-position is occupied by a hydrogen atom.<sup>21</sup> With **HL1** only one major product was obtained in all cases. To unambiguously determine the coordination mode of the triazole ring in these compounds the X-ray structural analysis of two compounds was performed. The crystallographic parameters are given in the experimental part. A projection of the structure of [Ru(*d*<sub>8</sub>-bipy)<sub>2</sub>(L1)]<sup>+</sup> is shown in Figure 3. The structural details obtained for [Ru(phen)<sub>2</sub>(L1)]<sup>+</sup> are very similar (see Figure S1). Selected bond lengths and angles are listed in Table 1. The data for the complexes [Ru(bipy)<sub>2</sub>(5Mptr)]PF<sub>6</sub>·4H<sub>2</sub>O<sup>22</sup> and [Ru(bipy)<sub>2</sub>(phenolptr)]PF<sub>6</sub>·CH<sub>3</sub>COCH<sub>3</sub><sup>23</sup> (see Figure 1) are added for comparison. In both, the pyridyltriazole ligand is coordinated via the *N2* atom of the triazole ring. The deprotonated state of the ring is confirmed by the presence of one PF<sub>6</sub><sup>-</sup> counter ion per ruthenium centre. The Ru-N distances and the bite angles for the compounds are similar to those observed for other similar compounds.<sup>24,25,26,27</sup> One significant difference between the two complexes is the position and orientation of the phenyl ring. In [Ru(phen)<sub>2</sub>(L1)]<sup>+</sup> the OMe unit at C2 is orientated away from the neighbouring 1,10-phenanthroline ligand, whereas in [Ru(*d*<sub>8</sub>-bipy)<sub>2</sub>(L1)]<sup>+</sup> it is orientated towards the coordinated 2,2'-bipyridine. This

corresponds to a rotation of the dimethoxy substituted phenyl ring around the C<sub>phenyl</sub>-C<sub>triazole</sub> bond. Both dimethoxy substituted phenyl rings are twisted out of plane of the pyridine triazole unit. For [Ru(*d*<sub>8</sub>-bipy)<sub>2</sub>(L1)]<sup>+</sup> the torsion angle is 20.8°, while for the phen compound a value of 25.9° is obtained. In the [Ru(*d*<sub>8</sub>-bipy)<sub>2</sub>(L1)]<sup>+</sup> solid-state structure there are several intermolecular hydrogen bonds. The oxygen of the methoxy group (labelled O2) serves as hydrogen bond acceptor for a water molecule (O2-O<sub>water</sub> = 2.971(10) Å). The same water molecule is also a hydrogen bond donor for the N6 atom of the triazole ring of a neighbouring molecule (N6-O<sub>water</sub> = 2.863(10) Å). This supramolecular association leads to the formation of one-dimensional chains consisting of alternating ruthenium complexes and water molecules and these chains are stacked upon each other as depicted in Figure 4. The resulting packing diagram is shown in Figure 5. [Ru(phen)<sub>2</sub>(L1)]<sup>+</sup> contains no water molecules even though the complex was obtained in an identical manner as [Ru(*d*<sub>8</sub>-bipy)<sub>2</sub>(L1)]<sup>+</sup>. In the solid state relatively weak intermolecular CH-N hydrogen bonds can be observed. N5 of the triazole moiety serves as hydrogen bond acceptor for a C5-H bond of a phenanthroline from a neighbouring complex (C5B-N5 = 3.285(10) Å, angle C5B-H5B-N5 = 139.9(3)). In both molecular structures no significant influence of the hydrogen bonding network on the coordination geometry can be observed.

### <sup>1</sup>H NMR Spectroscopy.

The <sup>1</sup>H NMR data for the complexes are listed in the experimental section. The resonances observed for the bipy and phen ligands are as expected and are not included. The assignment of the signals was carried out with the help of 2D <sup>1</sup>H COSY spectra and the use of partial deuteration of the complexes (See Figure 6). These spectra clearly show the presence of only one isomer. Figure 6b shows that selective deuteration greatly simplifies the spectra. From this spectrum the deuteration of the phen ligands is estimated to be better than 95%. The quantitative demethylation of [Ru(bipy)<sub>2</sub>(L1)]<sup>+</sup> and [Ru(phen)<sub>2</sub>(L1)]<sup>+</sup> to form [Ru(bipy)<sub>2</sub>(L2)]<sup>+</sup> and [Ru(phen)<sub>2</sub>(L2)]<sup>+</sup> respectively, can be verified by the absence of the -OMe resonances between 3.7 and 3.9 ppm. In addition, there are also small but significant changes in the position of the proton resonances for the coordinated **L2**<sup>+</sup> moiety compared to the methoxy precursor ligand. Proton resonances for the deprotected ligand are shifted to higher field by about 0.1-0.2 ppm. The effect is largest for the phenyl protons.

### Electronic and Photophysical properties.

UV-Visible spectra of the complexes are consistent with those observed for other pyridyltriazole compounds<sup>5,22,28</sup> and are listed in Table 2. The spectra are dominated in the visible region (300-500 nm) by dπ-π\* metal-to-ligand-charge-transfer (MLCT) transitions, while the UV spectrum is dominated by intense π-π\* transitions associated with the different ligands. On protonation of the triazole ring the <sup>1</sup>MLCT absorption bands of the complexes undergo a blue shift (see Table 2) as a result of the reduced electron donor properties of the triazole ring.

All compounds exhibit emission at 298 K with the λ<sub>max</sub> of the deprotonated complexes occurring at lower energy than observed for [Ru(bipy)<sub>3</sub>]<sup>2+</sup> (605 nm).<sup>29</sup> This is explained by the strong σ-donor properties of the anionic triazole ligand. As with the absorption spectra, protonation of the triazole ring in the complexes results in a blue shift of the emission maxima. The emission lifetimes of the deprotonated species are listed in Table 2. The lifetimes of the protonated species are <10 ns (i.e. shorter than the limit of the detection system employed). The lifetimes obtained for [Ru(phen)<sub>2</sub>(L1)]<sup>+</sup> and [Ru(*d*<sub>8</sub>-phen)<sub>2</sub>(L1)]<sup>+</sup> are considerably longer than those found for the analogous bipy-

based compounds. The significant increase in emission lifetime upon deuteration<sup>30</sup> of the bipy and phen ligands, from 70 to 90 ns and from 365 to 500 ns respectively, suggests that the emitting state is based on the polypyridyl ligands rather than the pyridyl-triazole based ligands.<sup>31</sup> The emission lifetime of  $[\text{Ru}(\text{bipy})_2(\text{L1})]^+$  and  $[\text{Ru}(\text{bipy})_2(\text{L2})]^+$  are very similar (See Table 2). However, the lifetime observed for  $[\text{Ru}(\text{phen})_2(\text{L2})]^+$  (225 ns) is shorter than found for  $[\text{Ru}(\text{phen})_2(\text{L1})]^+$  (365 ns). This suggests that there is a significant quenching by the catechol moiety in the phen analogue, most likely via an electron transfer mechanism. A comparison of the two lifetimes suggests that the quenching rate is about  $2 \times 10^6 \text{ s}^{-1}$ .<sup>32</sup> This relatively slow rate would be expected to have a limited effect on the short (70 ns) lifetime of  $[\text{Ru}(\text{bipy})_2(\text{L1})]^+$ . A detailed study on the photophysical properties of these and of related hydroquinone (HL3, see Figure 1) compounds is in progress.

### Acid-base properties.

The effect of protonation and deprotonation of the triazole ring on the  $\lambda_{\text{max}}$  of absorption and emission spectra is illustrated in Table 2. The acid-base behaviour of the compounds was studied by recording the pH dependence of these spectra. A typical ground-state titration is shown in Figure 7. For all compounds clear isosbestic points are observed and all changes are reversible in the pH range 1-8. However in the pH range 8-12, under aerobic conditions, the spectroscopic changes observed for  $[\text{Ru}(\text{bipy})_2(\text{L2})]^+$  and  $[\text{Ru}(\text{phen})_2(\text{L2})]^+$  are not reversible probably because of the formation of semiquinone intermediates. The  $pK_a$  values obtained for the coordinated triazole ring are shown in Table 2. Information about the excited state acidity can be obtained from the pH dependence of the emission spectra. A typical titration showing the pH dependence of the emission of  $[\text{Ru}(\text{phen})_2(\text{L2})]^+$  is shown in the supplementary material as Figure S2. The changes observed may allow for determination of the location of the excited state.<sup>33</sup> Excited state  $pK_a^*$  values ( $pK_a^*$ ) were evaluated using the Förster method<sup>34</sup> as shown in equation 1;

$$pK_a^* = pK_a + (0.625/T)(v_B - v_{HB}) \quad (1)$$

where  $v_B$  and  $v_{HB}$  are the  $E_{0-0}$  values (in  $\text{cm}^{-1}$ ) of the deprotonated and protonated complexes respectively. These values are taken from the  $\lambda_{\text{max}}$  of the emission spectra at 77 K as they are the most accurate means of obtaining an estimate for the energy difference involved in the 0-0 transitions. This equation gives an estimate of the excited state acidity of the compound. A more reliable method is based on the measurement of the emission lifetimes of both the protonated and the deprotonated species.<sup>34</sup> However, for the compounds reported here the emission of the protonated compounds is well below 10 ns, which prevents the formation of equilibrium in the excited state. This lack of equilibrium in the excited state limits the physical meaning of the  $pK_a^*$  values obtained using equation 1. The trend observed is nevertheless significant and the increased acidity in the excited state indicates that formation of the <sup>3</sup>MLCT excited state involves transfer of charge from Ru(II) to a polypyridyl rather than the triazole based ligand.<sup>33,35</sup> This observation is in agreement with the dependence of the emission lifetime on deuteration as outlined above.

### Electrochemical Properties.

**Complexes based on the HL1 ligand.** The oxidation and reduction potentials of the complexes are presented in Table 2. Between 0 V to 1.0 V vs Ag/AgCl the complexes  $[\text{Ru}(\text{bipy})_2(\text{L1})]^+$  and  $[\text{Ru}(\text{phen})_2(\text{L1})]^+$  feature a reversible oxidation process at  $\sim 0.8$  V vs Ag/AgCl (see Figure 8). An irreversible oxidation is observed at potentials close to 1.2 V. To further investigate the nature of these two redox processes spectroelectrochemical measurements were carried out. Bulk

oxidation of  $[\text{Ru}(\text{bipy})_2(\text{L1})]^+$  at 1.00 V vs Ag/AgCl leads to the appearance of new bands in the region 400-1600 nm. The analogous  $[\text{Ru}(\text{phen})_2(\text{L1})]^+$  complex shows similar results. The new bands have been assigned as ligand-to-metal charge transfer (LMCT) bands on the basis of their energy and intensity and by comparison with structurally related complexes.<sup>35,36,37</sup> The expected depletion of <sup>1</sup>MLCT absorption bands is masked by the concomitant growth of bands at 435, 478 and 1167 nm for the bipy complex (see Figure 9) and 420 and 1166 nm for the phen complex. A full recovery of the original spectrum was observed upon electrochemical reduction of the oxidised species, confirming the reversibility of the first oxidation process and allowing it to be attributed to a metal centred oxidation process. Oxidation at potentials above 1.2 V results in further changes in the absorption spectrum. These changes are however irreversible and therefore no further detailed electrochemical experiments were carried out. The irreversibility of the second oxidation process suggests that this process is related to the presence of methoxy groups.<sup>5</sup> This assignment is further addressed in the calculation section below.

The LMCT spectra of Ru(III) complexes have received relatively little attention, in part due to their low intensity (*e.g.*  $\epsilon \leq 500 \text{ M}^{-1}\text{cm}^{-1}$  for  $[\text{Ru}(\text{bipy})_3]^{2+}$ ) and also because of their non-emissive nature. It is clear, however that both the energy and intensity of LMCT bands can vary greatly,<sup>38</sup> with a direct correlation between the  $\sigma$ -donor strength of the ligands and band intensity. LMCT bands of moderate intensity in the red/near IR region have previously been observed in the mixed-ligand complexes of Ru(III) containing electron-rich donor ligands such as bisbenzimidazole<sup>39</sup> and bispyridinetriazoles.<sup>36</sup> The position and intensity of these LMCT bands correlate well with those found here. The intense LMCT bands for  $[\text{Ru}(\text{bipy})_2(\text{L1})]^{2+}$  and  $[\text{Ru}(\text{phen})_2(\text{L1})]^{2+}$  complexes are, therefore, not unexpected considering the electron rich nature of the deprotonated triazole ligand.

In related complexes, protonation of the triazole ring shifts the reversible metal based oxidation about 400 mV more positive.<sup>5a</sup> Surprisingly Figure 8 shows that the anodic shift is less than expected and also that an irreversible signal is obtained. The lack of reversibility observed for the oxidation process upon protonation of the ligand is possibly best explained by an overlap between the, still reversible, metal oxidation and the irreversible methoxy based redox process. The ZINDO calculations do indeed indicate that the methoxy and metal-based oxidation processes are expected to be much closer when the triazole is protonated. (*vide infra*) Unfortunately the irreversibility of the redox wave and in particular fouling of the electrode did prevent more detailed studies. The reduction waves observed are by comparison with other polypyridyl complexes assigned to bipy or phen based reductions.<sup>5</sup> The reduction processes are not well defined due to surface adsorption effects and become irreversible by protonation and deprotonation effects initiated by the reduction processes.<sup>40</sup> This prevents a detailed investigation of the reduction processes.

**Complexes based on the HL2 ligand** The cyclic voltammogram of the complex  $[\text{Ru}(\text{bipy})_2(\text{L2})]^+$  is shown in Figure 10. Between 0.0 and 1.4 V vs Ag/AgCl the compound shows three oxidation waves and a number of poorly defined reduction processes. None of the processes appear reversible but considering the complexity of the hydroquinone/quinone redox couple this is not unexpected. Several attempts were made to improve the quality of the CV. One approach involved pre-treatment of the electrode as described by Cabaniss et al.<sup>41</sup> This treatment involves anodisation of the glassy carbon electrode by placing it in 0.1 M  $\text{H}_2\text{SO}_4$  at a potential of 1.80 V for 1 minute. This did not significantly improve the behaviour obtained and the results reported in Figure 10 are the best obtained. Similar problems

were observed for the oxidative chemistry of the analogous complex  $[\text{Ru}(\text{bipy})_2(\text{L3})]^+$  (see Figure 1). However, for this compound electrode anodisation led to a much improved CV and three well-defined redox processes were observed in the anodic region. Based on spectroelectrochemical investigations, the first process at 0.74 V was assigned to the oxidation of the hydroquinone group to the semiquinone species. The result of this oxidation process is that the adjacent triazole group is protonated. This results in a quasi-reversible oxidation wave with a  $E_{1/2}$  of 1.18V. The semiquinone/quinone oxidation is observed at 1.01 V. The pattern observed for  $[\text{Ru}(\text{bipy})_2(\text{L2})]^+$  and  $[\text{Ru}(\text{phen})_2(\text{L2})]^+$  is not unlike that observed for  $[\text{Ru}(\text{bipy})_2(\text{L3})]^+$  but as expected the electrochemistry of the catechol grouping is much less well-defined.<sup>42</sup> As a result spectroelectrochemical measurements did not yield unambiguous results. It seems likely however that the redox waves observed at 0.82 and 1.00 V are best described as a two step oxidation of the catechol moiety of the ligand **HL2** to the quinone. The last oxidation step at 1.22 V is best explained by the oxidation of the quinone complex in which the triazole ring is protonated. This process is not expected to be intramolecular in nature as proposed for  $[\text{Ru}(\text{bipy})_2(\text{L3})]^+$ , but is most likely caused by an increase in the acidity of the solution following proton release upon oxidation of the catechol ring.

### Calculations.

To better understand the electrochemical behaviour of the methoxy compounds the electronic structures of  $[\text{Ru}(\text{bipy})_2(\text{HL1})]^{2+}$  and  $[\text{Ru}(\text{bipy})_2(\text{L1})]^+$ , were calculated using ZINDO/S. The structures of both complexes were geometry optimised before ZINDO/S calculations were performed. The ZINDO/1 optimised structure of this compound shows good agreement with the x-ray structure reported for the  $d_8$ -bipy analogue discussed above. For the protonated complexes, protonation may occur either at the *N1* or *N4* position of the triazole ring. ZINDO/S calculations on each isomer gave very similar results. The results for the *N4* isomer will be discussed here. The HOMO and LUMO levels of  $[\text{Ru}(\text{bipy})_2(\text{HL1})]^{2+}$  and  $[\text{Ru}(\text{bipy})_2(\text{L1})]^+$  are shown in Figure 11, with corresponding information on their relative energies and atomic orbital contributions. Values for atomic orbital contributions of the pyridyltriazole (*pytrz*), and dimethoxyphenyl (*ph*), moieties of L1 have been determined separately.

The HOMO of the deprotonated complex contains significant contributions from each of the ligand and metal-based components considered in the calculation. However, the value for *ph* is about one-third of that for the *pytrz* portion (11% vs. 30%). This situation is changed in the protonated complex, where the contribution of the *ph* moiety to the HOMO is slightly greater than that of *pytrz* (29% vs. 25%). The metal centre contributes equally to the HOMOs of both complexes. The LUMO of the deprotonated complex is almost completely bipy-based (88%). On protonation, both bipy and *pytrz* make a 50:50 contribution to the LUMO.

Calculated density of states (DOS) spectra have been shown to be a useful method to visualise the spatial distribution of the electronic structure of complexes.<sup>43</sup> In particular, where there are several close-lying energy levels in the frontier region, DOS spectra give a better picture of the contributions of the various moieties to the HOMO and LUMO, compared to examination of individual energy levels.

DOS spectra calculated for  $[\text{Ru}(\text{bipy})_2(\text{L1})]^+$  and its protonated form are shown in Figure 12. For the deprotonated form, we can clearly see that though the *ph* moiety makes a large contribution to H-2, H-3 and H-4, it contributes little to HOMO and H-1, which are somewhat separate in energy from the others. The

highest occupied molecular orbital levels of the protonated complex are closely spaced, resulting in a peak, which shows a large contribution from the Ru, and then similar contributions from the other three moieties though with *pytrz* contributing the least. On protonation, a significant difference in the LUMOs is apparent also. They change from bipy-based to having an equally large contribution from the bipy and *pytrz* moieties.

According to Koopmans' theorem, electrochemical oxidation of the complex is equivalent to the removal of an electron from the HOMO. The observed differences in the electrochemical behaviour of  $[\text{Ru}(\text{bipy})_2(\text{HL1})]^{2+}$  and  $[\text{Ru}(\text{bipy})_2(\text{L1})]^+$  agree qualitatively with the calculated differences in their electronic structures. The calculations show the electronic structure of the highest occupied molecular orbitals to be that of a typical triazole, containing significant contributions from the metal centre, bipy and *pytrz* moieties. Experimentally a reversible peak at 0.8V is found due to the oxidation of the metal centre. On protonation, it is found that the methoxy group is oxidised at a potential close to that of the expected oxidation potential of the metal. The DOS spectra support these results, showing that the *ph* moiety makes a significant contribution to the highest occupied molecular orbitals on protonation of the complex.

### Concluding remarks.

The results obtained show that deprotection of dimethoxy precursors is an effective route to the synthesis of ligands containing catechol type pending groups. The spectroscopic, electrochemical and acid-base properties of the compounds obtained are in agreement with those obtained for ruthenium compounds based in similar pyridyltriazole ligands. Electrochemical evidence seems to suggest that upon oxidation of the catechol group a partial protonation of the triazole moiety takes place. ZINDO calculations provide a good qualitative description of the electronic properties of the methoxy compounds and confirm the assignments made for the two oxidations observed at ~1.0 V. This highlights the usefulness of ZINDO type calculations in the investigation of ruthenium polypyridyl complexes. The emission lifetime data suggest that although the interaction between the hydroquinone group and the polypyridyl based excited state is weak, the change in lifetime observed for the phen analogue is significant. Based on the redox properties of the hydroquinone grouping it seems most likely that this quenching is caused by a photoinduced electron transfer process. At present further photophysical studies are taking place, investigating the properties of the catechol complexes. Preliminary results have shown that the catechol moiety can bind a range of first row transition metal ions and that binding can strongly effect the emitting properties of the ruthenium core. The compounds have therefore potential applications as metal ion sensors and can act as models for the investigation of photoinduced energy and electron transfer reactions. Results on these studies will be reported in a subsequent paper.

### Acknowledgements.

This research was partly funded by Enterprise Ireland and the European Communities Programmes, Training and Mobility of Researchers, under Contract 96CT-0076 and the Human Potential Programme under Contract HPRN-CT-2002-00185.

## Table legends

Table 1	Selected bond distances (Å) and angles (°) of $[\text{Ru}(d_8\text{-bipy})_2(\text{L1})]^+$ and $[\text{Ru}(\text{phen})_2(\text{L1})]^+$ and some related compounds.
Table 2	Spectroscopic and electrochemical data for complexes described in text and related complexes.
Supplementary Material	
Table S1	Energy and % contribution of atomic orbitals to each molecular orbital in the frontier region for (a) $[\text{Ru}(\text{bipy})_2(\text{L1})]^+$ and (b) $[\text{Ru}(\text{bipy})_2(\text{HL1})]^{2+}$ . The contribution of both <b>HL1</b> and <b>L1</b> <sup>+</sup> , the protonated and the deprotonated pyridyltriazole ligands, is divided into a pyridinetriazole component, <i>pytrz</i> and a contribution from the dimethoxyphenyl moiety, <i>ph</i> .

## Figure Legends.

Figure 1.	Structures and labelling scheme for <sup>1</sup> H NMR of ligands.
Figure 2.	<i>N2</i> and <i>N4</i> binding modes in complexes described in text.
Figure 3.	Molecular structure of $[\text{Ru}(d_8\text{-bipy})_2(\text{L1})]^+$ showing atomic numbering. (N.B. the crystallographic atom labelling scheme is different to that employed in the text to refer to the coordination mode of the 1,2,4-triazole, see Figure 2)
Figure 4.	Schematic representation of the inter-molecular interaction in $[\text{Ru}(d_8\text{-bipy})_2(\text{L1})]^+$ .
Figure 5.	Packing diagram for $[\text{Ru}(d_8\text{-bipy})_2(\text{L1})]^+$ .
Figure 6.	<sup>1</sup> H-NMR spectrum in <i>d</i> <sub>3</sub> -acetonitrile of a) $[\text{Ru}(\text{phen})_2(\text{L1})]^+$ and b) $[\text{Ru}(d_8\text{-phen})_2(\text{L1})]^+$ .
Figure 7.	pH dependence of the absorption spectrum of $[\text{Ru}(\text{bipy})_2(\text{L2})]^+$ ( $5 \times 10^{-5}$ M) in an aqueous Britton-Robinson buffer at pH 1.44, 1.79, 2.09, 2.55, 2.95, 3.13, 3.70, 4.18, 4.92 and 6.66.
Figure 8.	Cyclic voltammogram of a) $[\text{Ru}(\text{bipy})_2(\text{L1})]^+$ and b) $[\text{Ru}(\text{bipy})_2(\text{HL1})]^{2+}$ ( $1 \times 10^{-3}$ M) in acetonitrile with 0.1 M TEAP (A few drops of TFA were added to ensure protonation of the triazole ring.) (Scan rate: 100 mV s <sup>-1</sup> ).
Figure 9.	Spectroelectrochemistry of $[\text{Ru}(\text{bipy})_2(\text{L1})]^+$ in acetonitrile with 0.1 M TEAP at 0 V, 1.00 V and 1.50 V vs Ag/AgCl (ordinate axis is set on non-linear scale for clarity).
Figure 10.	Cyclic voltammogram of $[\text{Ru}(\text{bipy})_2(\text{L2})]^+$ ( $1 \times 10^{-3}$ M) in acetonitrile with 0.1 M TEAP (Scan rate: 100 mVs <sup>-1</sup> ).
Figure 11.	Isosurface drawings of the HOMO and LUMO levels of (a) $[\text{Ru}(\text{bipy})_2(\text{L1})]^+$ in which the triazole ring is deprotonated and (b) $[\text{Ru}(\text{bipy})_2(\text{HL1})]^{2+}$ , in which the triazole ring is protonated. Also shown are the energies of the levels in eV and the % contribution of the metal and ligands to the molecular orbital, based on the contributions of the individual atomic orbitals to the molecular orbital. The contribution of both <b>HL1</b> and <b>L1</b> <sup>+</sup> , the protonated and the deprotonated pyridyltriazole ligands, is divided into a pyridinetriazole component, <i>pytrz</i> and a contribution from the dimethoxyphenyl moiety, <i>ph</i> .
Figure 12.	Calculated density of states (DOS) diagram showing contributions from the metal centre, the ligands for (a) $[\text{Ru}(\text{bipy})_2(\text{L1})]^+$ in which the triazole ring is deprotonated and (b) $[\text{Ru}(\text{bipy})_2(\text{HL1})]^{2+}$ , where the triazole ring is protonated. The contribution of both <b>HL1</b> and <b>L1</b> <sup>+</sup> , the protonated and the deprotonated pyridyltriazole ligands, is divided into a pyridinetriazole component, <i>pytrz</i> and a contribution from the dimethoxyphenyl moiety, <i>ph</i> . The contributions are shown stacked upon one another. The bars at the bottom of each graph represent the ZINDO/S calculated energy levels. See text for details.

Supplementary material.

Figure S1. Molecular structure of  $[\text{Ru}(\text{phen})_2(\text{L1})]^+$  showing atomic numbering.

Figure S2. pH dependence of the emission spectrum of  $[\text{Ru}(\text{phen})_2(\text{L2})]^+$  ( $5 \times 10^{-5}$  M) in an aqueous Britton-Robinson buffer at pH 1.72, 2.11, 2.32, 2.84, 3.22, 3.53, 3.85, 4.11, 5.28 and 6.15.

**Table 1** Selected bond distances (Å) and angles (°) of [Ru(*d<sub>s</sub>*-bipy)<sub>2</sub>(L1)]<sup>+</sup> and [Ru(phen)<sub>2</sub>(L1)]<sup>+</sup> and some related compounds.

	<b>Bond distances (Å)</b>			
	[Ru( <i>d<sub>s</sub></i> -bipy) <sub>2</sub> (L1)] <sup>+</sup>	[Ru(phen) <sub>2</sub> (L1)] <sup>+</sup>	<b>Ru5Mptr<sup>a</sup></b>	<b>Rupt<sup>a</sup></b>
<b>Ru - N4</b>	2.038(4)	2.036(4)	2.050(5)	2.051(3)
<b>Ru - N3</b>	2.109(4)	2.089(4)	2.086(4)	2.085(3)
<b>Ru - N1B</b>	2.044(4)	2.057(4)	2.055(4)	2.056(3)
<b>Ru - N2B</b>	2.044(4)	2.054(4)	2.042(5)	2.056(3)
<b>Ru - N2A</b>	2.043(4)	2.071(4)	2.060(4)	2.063(3)
<b>Ru - N1A</b>	2.062(4)	2.054(4)	2.056(4)	2.049(3)
	<b>Bond angles (°)</b>			
<b>N4 - Ru - N3</b>	77.86(15)	78.16(15)	78.0(2)	77.9(1)
<b>N4 - Ru - N1B</b>	94.29(15)	96.42(15)	96.1(2)	92.3(1)
<b>N4 - Ru - N1A</b>	96.11(15)	93.73(16)	96.5(5)	91.8(1)
<b>N4 - Ru - N2B</b>	89.88(15)	92.47(15)	87.4(2)	97.6(1)
<b>N3 - Ru - N2B</b>	96.25(17)	95.88(17)	95.0(2)	94.3(1)
<b>N3 - Ru - N2A</b>	94.88(15)	94.66(15)	95.9(2)	90.7(1)
<b>N3 - Ru - N1A</b>	86.28(15)	90.17(16)	90.9(2)	96.3(1)
<b>N1B - Ru - N2B</b>	79.00(17)	79.86(17)	79.4(2)	79.9(1)
<b>N1B - Ru - N2A</b>	93.29(15)	91.19(15)	90.5(2)	97.8(1)
<b>N2B - Ru - N2A</b>	95.48(16)	94.59(16)	98.0(2)	90.9(1)
<b>N2A - Ru - N1A</b>	78.73(16)	79.83(15)	78.7(2)	78.7(1)

<sup>a</sup> **Ru5Mptr** = [Ru(bipy)<sub>2</sub>(5Mptr)]PF<sub>6</sub>·4H<sub>2</sub>O<sup>22</sup> and **Rupt** = [Ru(bipy)<sub>2</sub>(phenolptr)]PF<sub>6</sub>·CH<sub>3</sub>COCH<sub>3</sub>.<sup>23</sup>

**Table 2** Spectroscopic and electrochemical data for complexes described in text and related complexes.

Complex	Abs <sup>a</sup> λ <sub>max</sub> (logε)		Em <sup>a</sup> λ <sub>max</sub> nm <sup>b</sup> (τ ns)				<sup>c</sup> pK <sub>a</sub> (± 0.1)	<sup>c</sup> pK <sub>a</sub> * (± 0.1)	<sup>d</sup> Anodic E <sub>1/2</sub> /V	<sup>d</sup> Cathodic E <sub>1/2</sub> /V
	nm		Prot		Deprot					
	Prot.	Deprot	300 K	77 K	300 K	77K				
[Ru(bpy) <sub>3</sub> ] <sup>2+</sup> <sup>e</sup>		452			615(1100)				1.21	-1.38
[Ru(bpy) <sub>2</sub> (5Mprt)] <sup>+</sup>	438	467(3.92)	612	587	660	610	4.9	-	0.75	-1.52; -1.79
[Ru(bipy) <sub>2</sub> (L1)] <sup>+</sup>	435	482(4.00)	616	578	692(70)	618	4.1	1.7	0.71, 1.25 (irr)	-1.35, -1.56
[Ru( <i>d</i> <sub>8</sub> -bipy) <sub>2</sub> (L1)] <sup>+</sup>	440	478(4.00)	620	582	689(90)	617	4.2	2.2	0.71, 1.25 (irr)	-1.35, -1.57
[Ru(bipy) <sub>2</sub> (L2)] <sup>+</sup>	440	476(4.01)	622	577	689(65)	625	4.2	1.4	0.82,(irr) 1.00,(irr) 1.22 (irr)	-
[Ru(phen) <sub>3</sub> ] <sup>2+</sup> <sup>e</sup>		442			604(460)				1.35	-1.46
[Ru(phen) <sub>2</sub> (L1)] <sup>+</sup>	420	427(4.13)	607	569	681(365)	608	4.4	2.0	0.76, 1.25 (irr)	-1.48 (irr), -1.55 (irr)
[Ru( <i>d</i> <sub>8</sub> -phen) <sub>2</sub> (L1)] <sup>+</sup>	418	426(4.13)	607	570	680(500)	606	4.0	1.8	0.78	-1.49 (irr), -1.59 (irr)
[Ru(phen) <sub>2</sub> (L2)] <sup>+</sup>	418	426(4.13)	607	568	663(225)	609	4.0	1.5	0.86, 1.05, 1.24 (irr)	-

<sup>a</sup> All measurements at 300 K were performed in acetonitrile. <sup>b</sup> Values in brackets are emission lifetimes in ns. Samples for lifetime measurements were degassed using N<sub>2</sub>. The lifetimes of the protonated complexes are too short to be measured with the equipment available. All measurements at 77 K were performed in ethanol/methanol 4:1 v/v. <sup>c</sup>Ground- and Excited-state pK<sub>a</sub> values were obtained in Britton-Robinson buffer <sup>d</sup>Electrochemical data for deprotonated complexes in V vs Ag/AgCl in acetonitrile with 0.1 M TEAP (Scan rate: 100 mVs<sup>-1</sup>). <sup>e</sup> values obtained from ref 29a, no acid/base chemistry observed for these two compounds so protonation/deprotonation labels not relevant

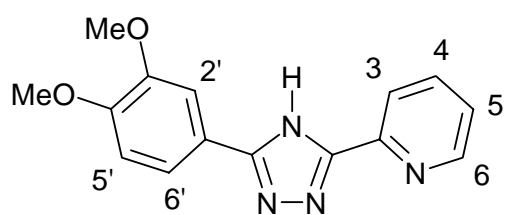
**Table S1** Energy and % contribution of atomic orbitals to each molecular orbital in the frontier region for (a)  $[\text{Ru}(\text{bipy})_2(\text{L1})]^+$  and (b)  $[\text{Ru}(\text{bipy})_2(\text{HL1})]^{2+}$ . The contribution of both **HL1** and **L1**, the protonated and the deprotonated pyridyltriazole ligands, is divided into a pyridinetriazole component, *pytrz* and a contribution from the dimethoxyphenyl moiety, *ph*.

(a) Deprotonated

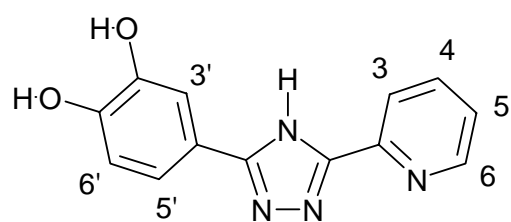
MO	eV	Ru	bipy1	bipy2	pytrz	ph
L+4	-2.95	4	60	19	17	0
L+3	-3.06	3	35	56	6	0
L+2	-3.30	5	8	22	65	0
L+1	-3.58	9	50	37	4	0
LUMO	-3.93	2	38	50	10	0
HOMO	-8.76	37	6	16	30	11
H-1	-9.15	57	20	10	13	0
H-2	-9.63	20	9	7	17	48
H-3	-10.00	72	7	6	5	9
H-4	-10.33	4	8	2	33	53

(b) Protonated

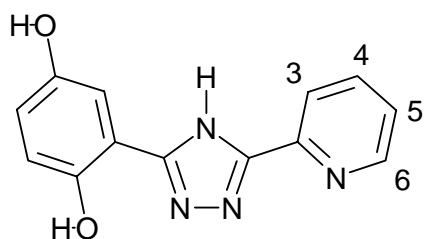
MO	eV	Ru	bipy1	bipy2	pytrz	ph
L+4	-5.26	2	23	8	66	1
L+3	-5.30	1	79	2	18	1
L+2	-5.97	8	9	74	9	0
L+1	-6.06	9	57	1	32	1
LUMO	-6.33	1	29	20	50	1
HOMO	-11.99	38	2	6	25	29
H-1	-12.22	69	15	13	3	0
H-2	-12.27	69	12	4	13	1
H-3	-12.43	29	2	5	5	60
H-4	-13.15	3	0	1	7	88



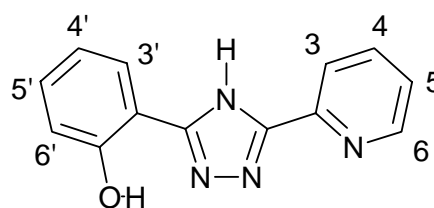
**HL1:** 2-[5-(3,4-dimethoxyphenyl)-4H-1,2,4-triazol-3-yl]pyridine



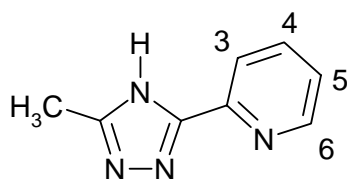
**HL2:** 4-(5-pyridin-2-yl-4H-1,2,4-triazol-3-yl)benzene-1,2-diol



**HL3:** 2-(5-pyridin-2-yl-4H-1,2,4-triazol-3-yl)benzene-1,4-diol

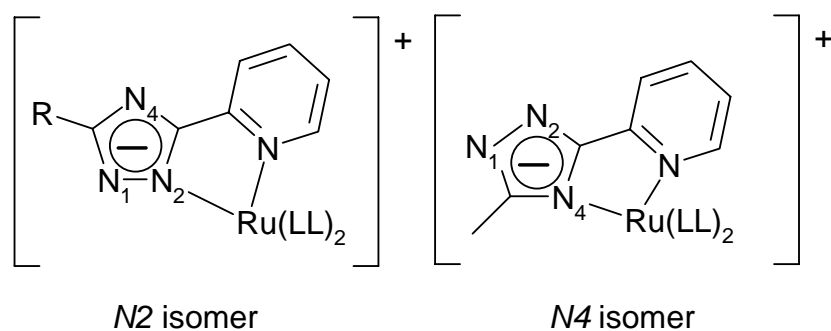


**Phenolptr:** 2-(5-Pyridin-2-yl-4H-1,2,4-triazol-3-yl)phenol



**5Mptr:** 2-(5-methyl-4H-1,2,4-triazol-3-yl)pyridine

**Fig. 1** Structures and labelling scheme for  $^1\text{H}$  NMR of ligands.



*N*2 isomer

*N*4 isomer

LL = 2,2'-bipyridine or 1,10-phenanthroline

**Fig. 2** *N*2 and *N*4 Binding modes in complexes described in text

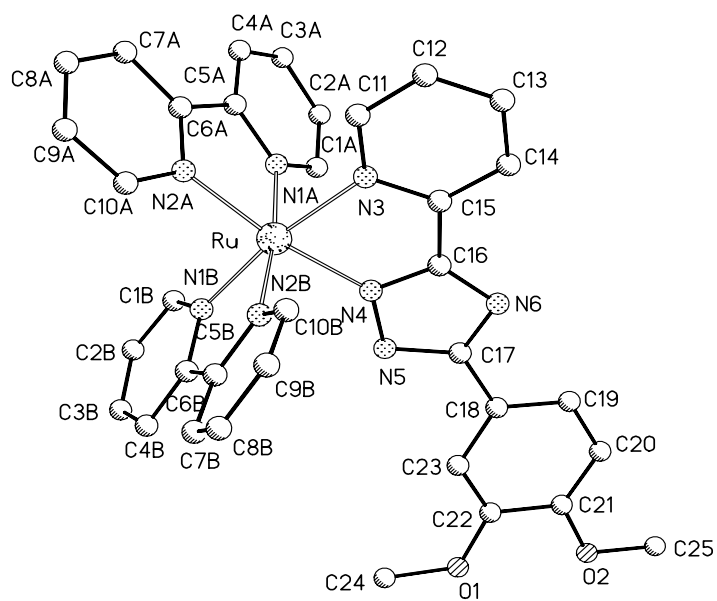


**Fig. 3** Molecular structure of  $[\text{Ru}(\text{ds-bipy})_2(\text{L1})]^+$  showing atomic numbering. (N.B. the crystallographic atom labelling scheme is different to that employed in the text to refer to the coordination mode of the 1,2,4-triazole, see Figure 2)

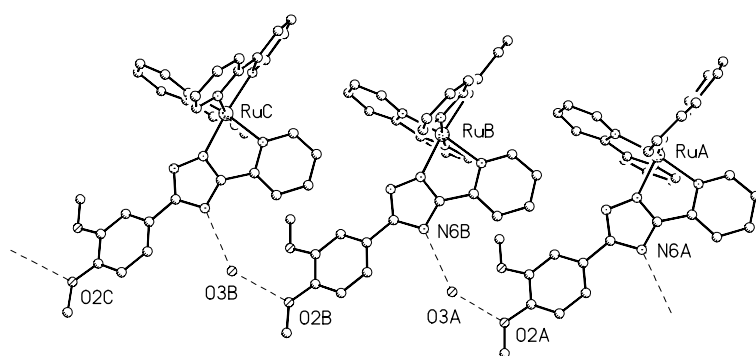


**Fig. 4** Schematic representation of the inter-molecular interactions in  $[\text{Ru}(\text{ds-bipy})_2(\text{L1})]^+$ .

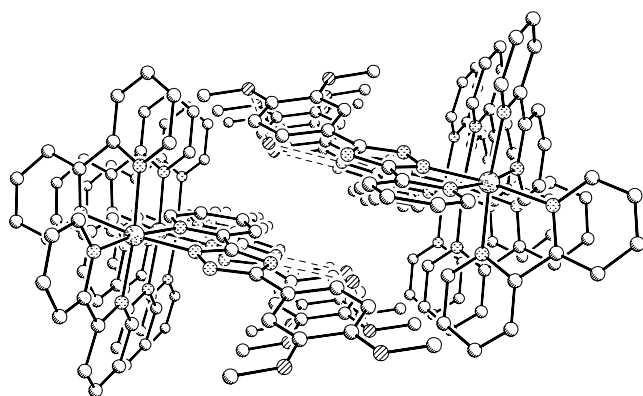


**Fig. 5** Packing diagram for  $[\text{Ru}(\text{ds-bipy})_2(\text{L1})]^+$

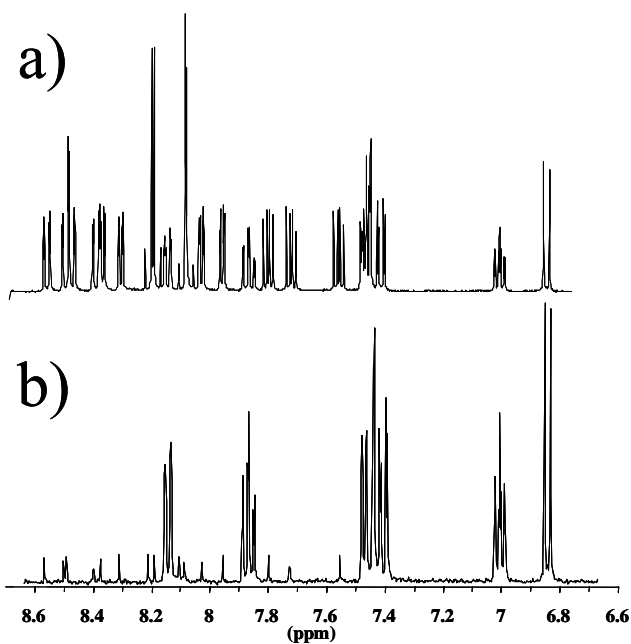


Fig. 6  $^1\text{H-NMR}$  spectrum in  $\text{d}_3$ -acetonitrile of a)  $[\text{Ru}(\text{phen})_2(\text{L1})]^+$  and b)  $[\text{Ru}(\text{d}_8\text{-phen})_2(\text{L1})]^+$ .

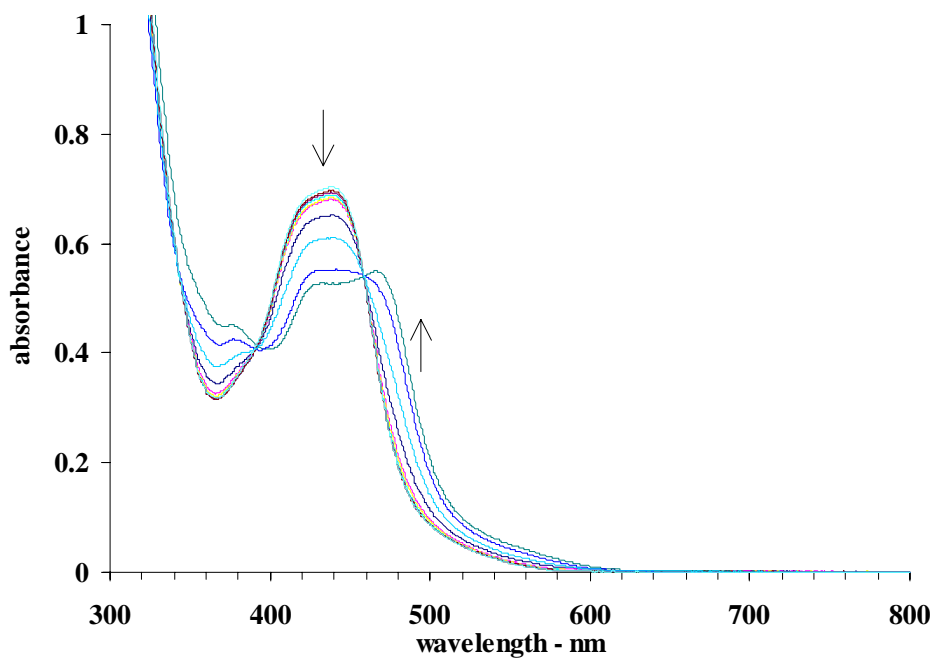
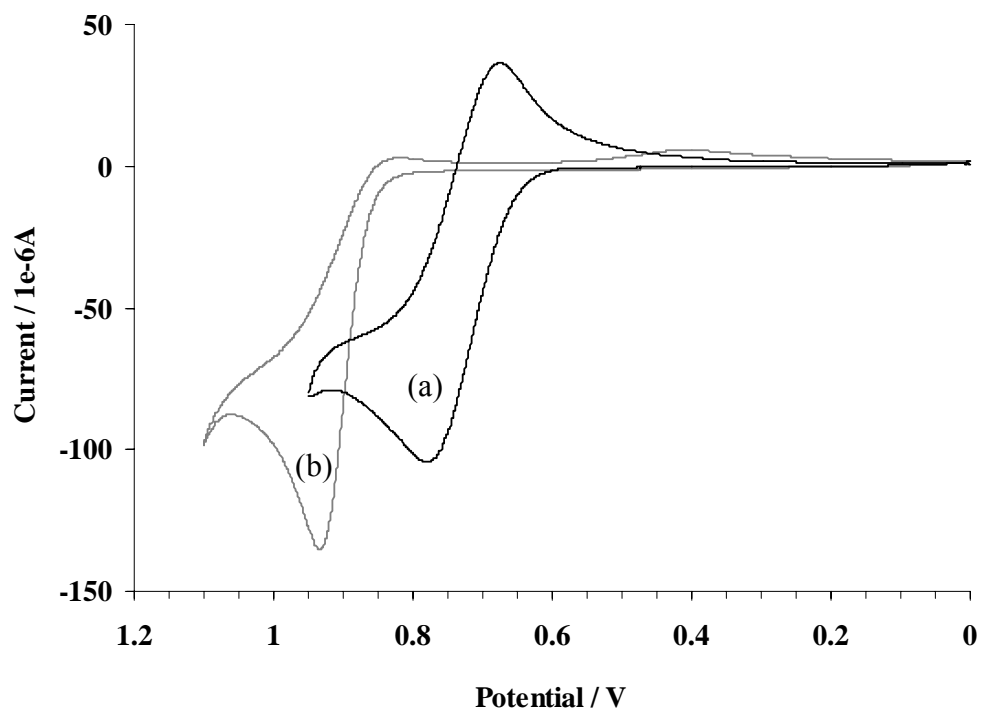
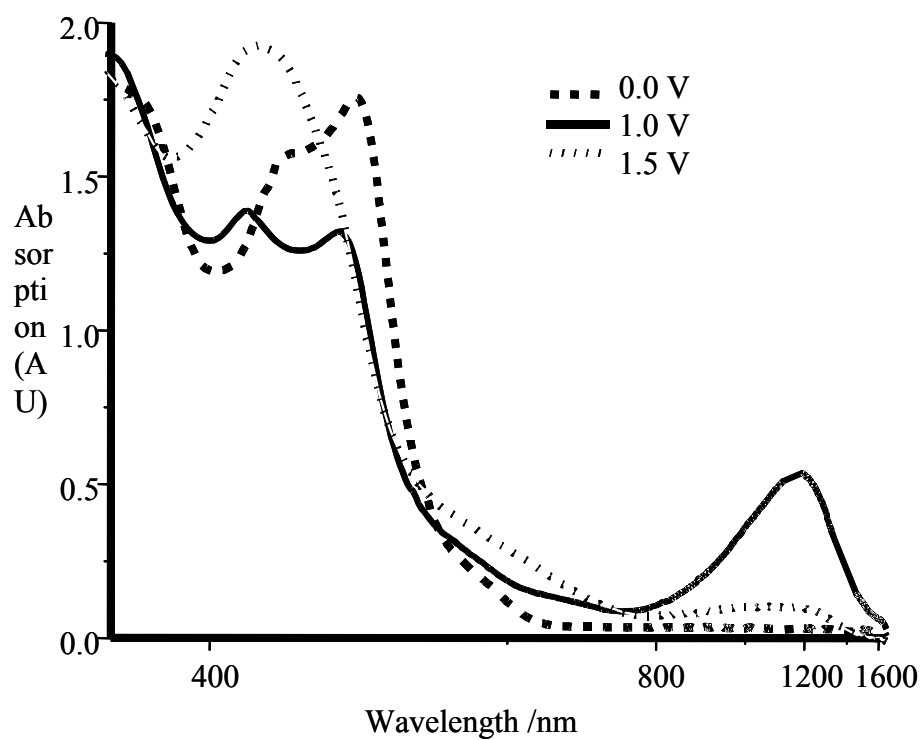


Fig. 7 pH dependence of the absorption spectra of  $[\text{Ru}(\text{bipy})_2(\text{L2})]^+$  ( $5 \times 10^{-5}$  M) in an aqueous Britton-Robinson buffer at pH 1.44, 1.79, 2.09, 2.55, 2.95, 3.13, 3.70, 4.18, 4.92 and 6.66.

**Fig. 8.** Cyclic voltammogram of a)  $[\text{Ru}(\text{bipy})_2(\text{L1})]^+$  and b)  $[\text{Ru}(\text{bipy})_2(\text{HL1})]^{2+}$  ( $1 \times 10^{-3}$  M) in acetonitrile with 0.1 M TEAP (A few drops of TFA were added to ensure protonation of the triazole ring.) (Scan rate:  $100 \text{ mV s}^{-1}$ ).





**Fig. 9** Spectroelectrochemistry of  $[\text{Ru}(\text{bipy})_2(\text{L1})]^+$  in acetonitrile with 0.1 M TEAP at 0 V, 1.00 V and 1.50 V vs Ag/AgCl (ordinate axis is set on non-linear scale for clarity).

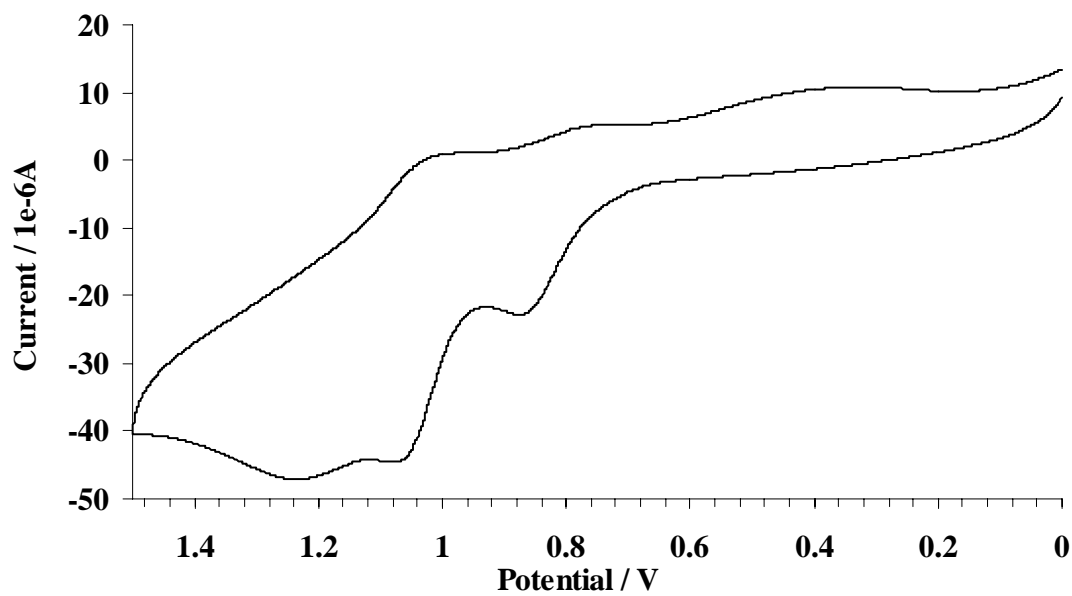


**Fig. 10** Cyclic voltammogram of  $[\text{Ru}(\text{bipy})_2(\text{L2})]^+$  ( $1 \times 10^{-3}$  M) in acetonitrile with 0.1 M TEAP (Scan rate:  $100 \text{ mVs}^{-1}$ ).

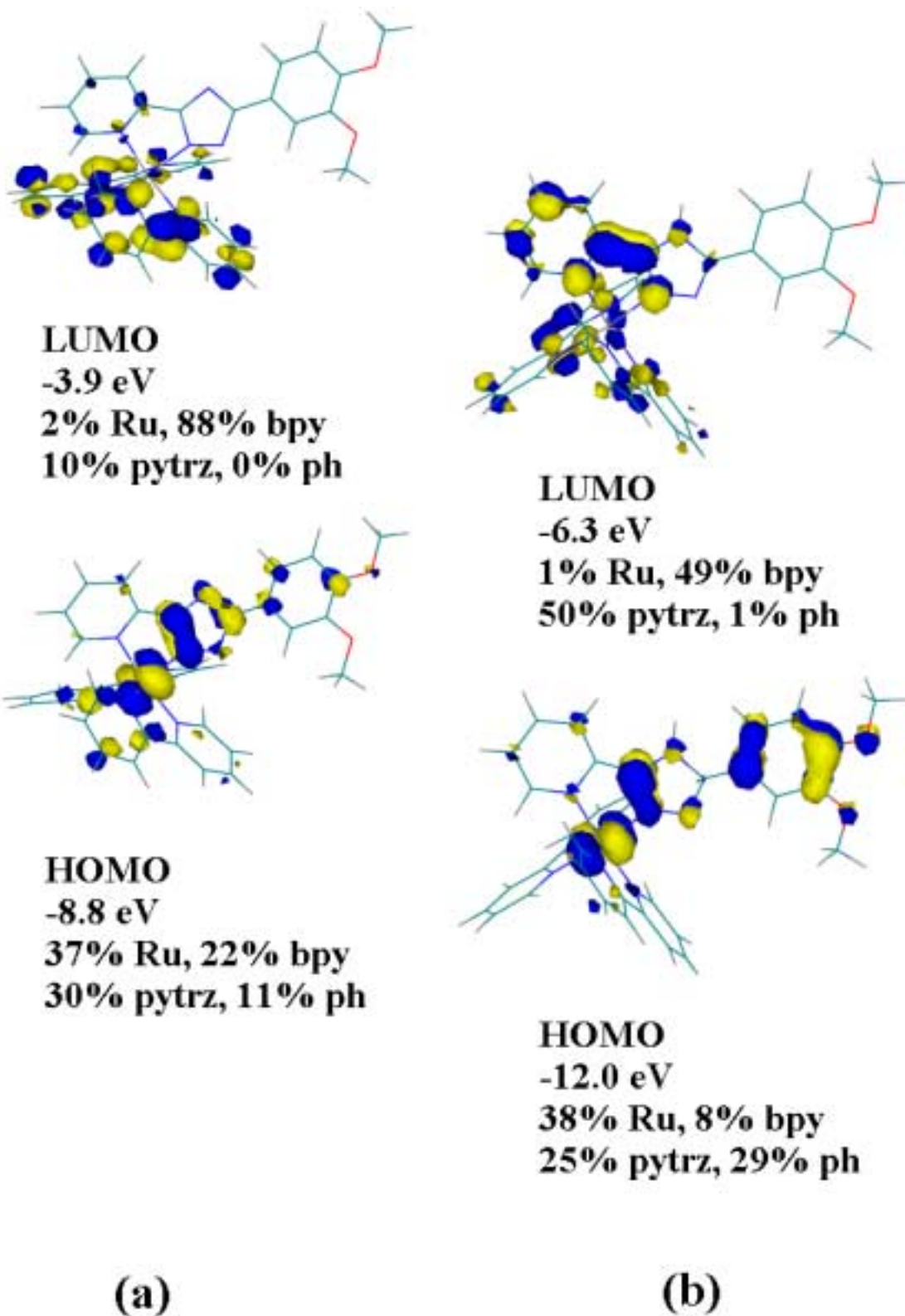
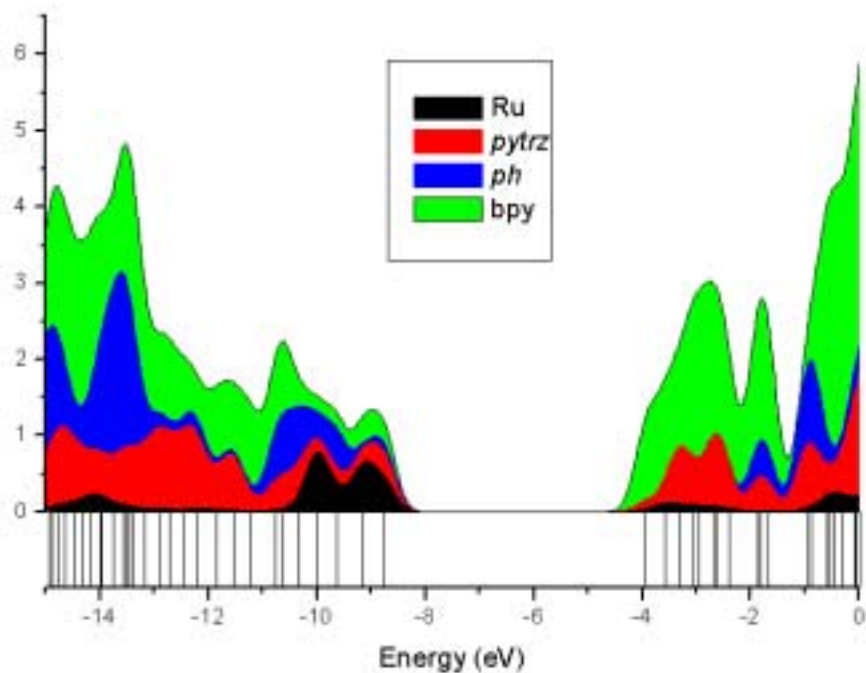
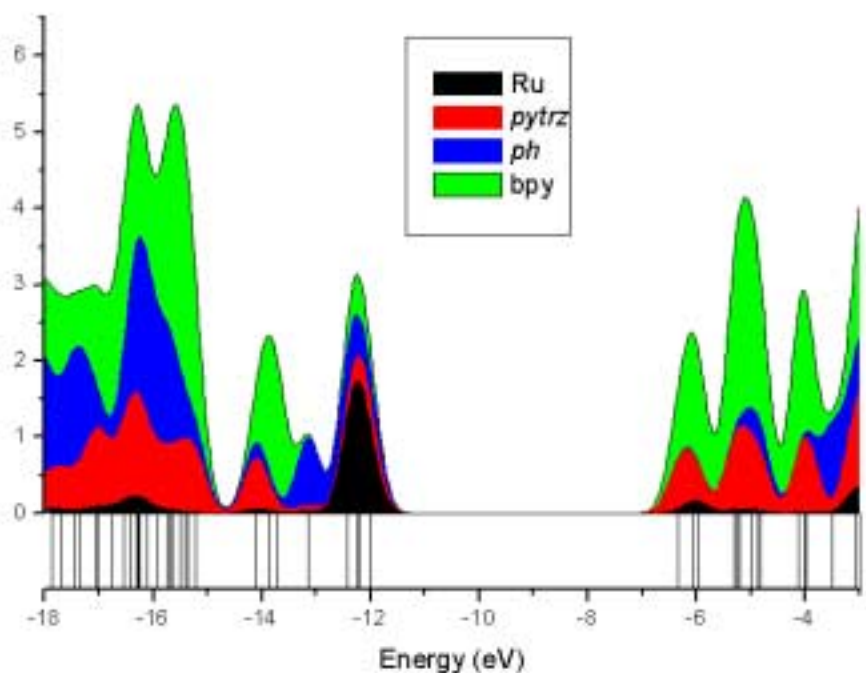


**Fig. 11** Isosurface drawings of the HOMO and LUMO levels of (a)  $[\text{Ru}(\text{bipy})_2(\text{L1})]^+$  in which the triazole ring is deprotonated and (b)  $[\text{Ru}(\text{bipy})_2(\text{HL1})]^{2+}$  in which the triazole ring is protonated. Also shown are the energies of the levels in eV and the % contribution of the metal and ligand to the molecular orbital, based on the contributions of the individual atomic orbitals to the molecular orbital. The contribution of both **HL1** and **L1**, the protonated and the deprotonated pyridyltriazole ligands, is divided into a pyridinetriazole component, *pytrz*, and a contribution from the dimethoxyphenyl moiety, *ph*.



**(a) Deprotonated**



**(b) Protonated**

**Fig. 12** Calculated density of states (DOS) diagram showing contributions from the metal centre, the ligands for (a)  $[\text{Ru}(\text{bipy})_2(\text{L1})]^+$  in which the triazole ring is deprotonated and (b)  $[\text{Ru}(\text{bipy})_2(\text{HL1})]^{2+}$ , where the triazole ring is protonated. The contribution of both **HL1** and **L1**, the protonated and the deprotonated pyridyltriazole ligands, is divided into a pyridinetriazole component, *pytrz* and a contribution from the dimethoxyphenyl moiety, *ph*. The contributions are shown stacked upon one another. The bars at the bottom of each graph represent the ZINDO/S calculated energy levels. See text for details.

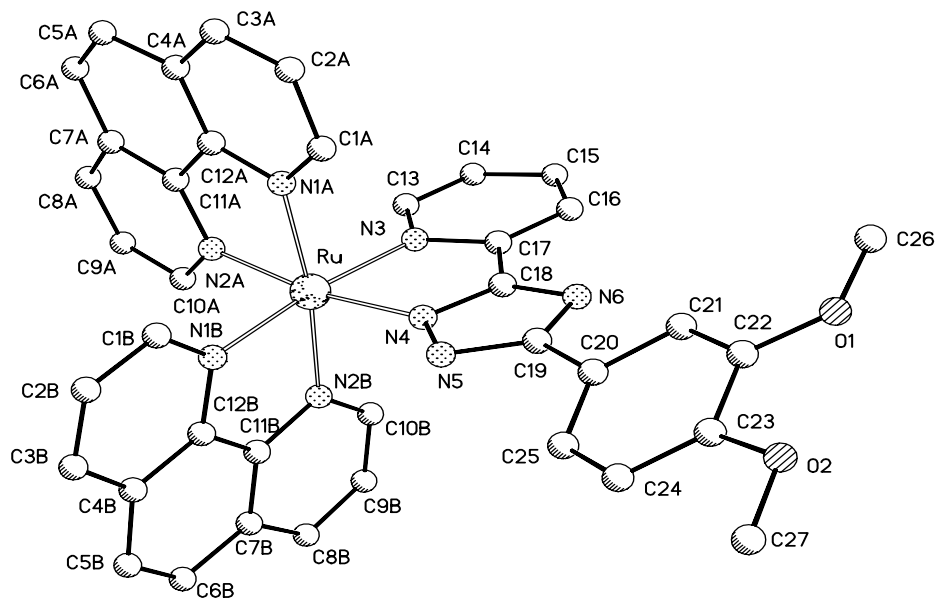


Fig. S1 Molecular structure of  $[\text{Ru}(\text{phen})_2(\text{L1})]^+$  showing atomic numbering.

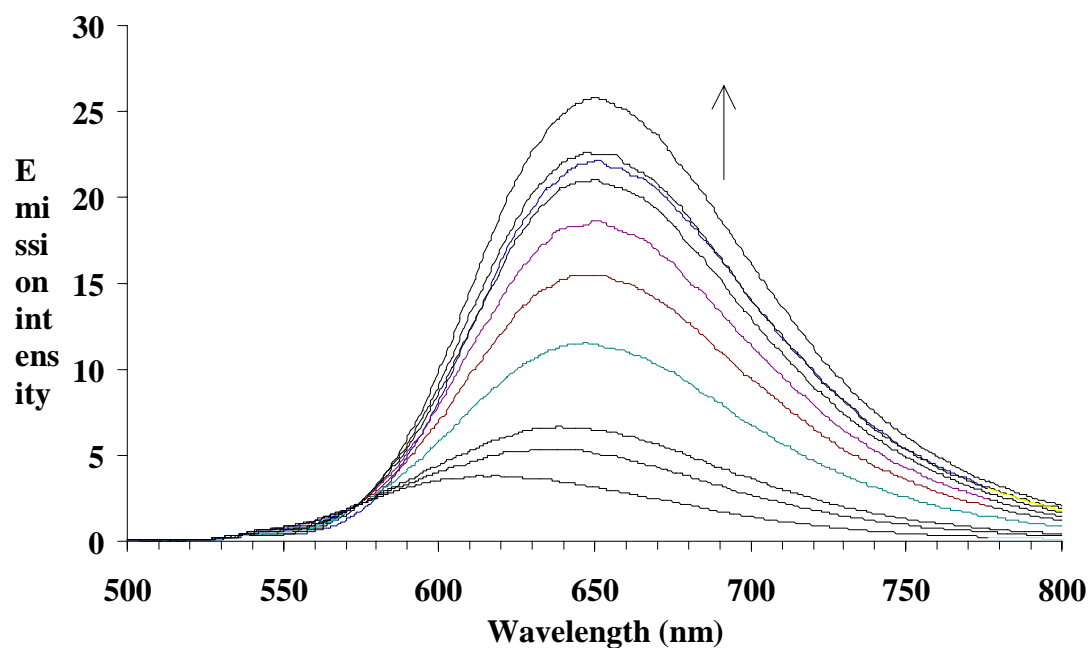


Fig. S2 pH dependence of the emission spectra of  $[\text{Ru}(\text{phen})_2(\text{L2})]^+$  ( $5 \times 10^{-5} \text{ M}$ ) in an aqueous Britton-Robinson buffer at pH 1.72, 2.11, 2.32, 2.84, 3.22, 3.53, 3.85, 4.11, 5.28 and 6.15.

- <sup>1</sup> R.K. Clayton, *Photosynthesis; Physical methods and chemical patterns*, 1st ed., Cambridge University Press, 1980.
- <sup>2</sup> (a) D. Gust, T.A. Moore, P.A. Liddell, G.A. Nemeth, L.R. Makings, A.L. Moore, D. Barrett, P.J. Pessiki, R.V. Benasson, M. Rougee, C. Chachaty, F.C. De Schryver, M. van der Auweraer, A.R. Hotzwarth, and J.S. Connolly, *J. Am. Chem. Soc.*, 1987, **109**, 846. (b) R. Foster and M. I. Foreman, in; *The Chemistry of Quinone compounds*, Ed. Spatai, Chapter 6, Wiley and Sons, Chichester, 1988.
- <sup>3</sup> M. Ebadi and A.B.P. Lever, *Inorg. Chem.* 1999, **38**, 467
- <sup>4</sup> V. Goulle, A. Harriman, J-M Lehn, *J. Chem. Soc. Chem. Commun.*, 1993, 1034.
- <sup>5</sup> (a) P. Passaniti, W. R. Browne, F. C. Lynch, D. Hughes, M. Nieuwenhuyzen, P. James, M. Maestri and J. G. Vos, *J. Chem. Soc. Dalton Trans.*, 2002, 1740. (b) F. M. Weldon and J. G. Vos. *Inorg. Chim. Acta*, 2000, **307**, 13.
- <sup>6</sup> R. Wang, T.E. Keyes, R. Hage, R.H. Schmehl, and J.G. Vos, *J. Chem. Soc., Chem. Commun.*, 1993, 1652.
- <sup>7</sup> W. R. Browne, C. M. O'Connor, J. S. Killeen, A. L. Guckian, M. Burke, P. James, M. Burke, and J.G. Vos, *Inorg. Chem.*, 2002, **41**, 4245.
- <sup>8</sup> B.P. Sullivan, D.J. Salmon, and T.J. Meyer, *Inorg. Chem.*, 1978, **17**, 3334.
- <sup>9</sup> (a) E.H. Vickery, L.F. Pahler and E.J. Eisenbraun, *J. Org. Chem.*, 1979, **44**, 4444. (b) J.F.W. McOmie, M.L. Watts and D.E. West, *Tetrahedron*, 1968, **24**, 2289. (c) B. Whittle, N.S. Everest, C. Howard, and M.D. Ward, *Inorg. Chem.*, 1995, **34**, 2025. (d) C.A. Howard and M.D. Ward, *Angew. Chem. Int. Ed. Engl.*, 1992, **31**, 1028.
- <sup>10</sup> (a) COLLECT, Data Collection Software; Nonius B.V., The Netherlands, 1998 (b) Z. Otwinowski and W. Minor, "Processing of X-Ray Diffraction Data Collected in Oscillation Mode", in *Methods in Enzymology*, Vol. 276, *Macromolecular Crystallography, Part A*, edited by C.W. Carter & R.M. Sweet, p 307, Academic Press 1997
- <sup>11</sup> G.M. Sheldrick, *Acta Crystallogr. Sect. A.*, 1990, **46**, 467.
- <sup>12</sup> G.M. Sheldrick, SHELXL-97 (Release 97-2), University of Göttingen, Germany, 1997.
- <sup>13</sup> CCDC 213441(phen complex) and 213442 (d<sub>8</sub>-bipy compound) contain the supplementary crystallographic data for this paper. These data can be obtained free of charge via [www.ccdc.cam.ac.uk/conts/retrieving.html](http://www.ccdc.cam.ac.uk/conts/retrieving.html) (or from the Cambridge Crystallographic Data Centre, 12, Union Road, Cambridge CB2 1EZ, UK; fax: (+44) 1223-336-033; or [deposit@ccdc.cam.ac.uk](mailto:deposit@ccdc.cam.ac.uk)).
- <sup>14</sup> HyperChem for Windows, Release 5.11 Standard Version, Hypercube, Inc., Gainesville, FL, USA, 1997
- <sup>15</sup> W. P. Anderson, T. R. Cundari, R. S. Drago, and M. C. Zerner, *Inorg. Chem.*, 1990, **29**, 1.
- <sup>16</sup> S. I. Gorelsky, E. S. Dodsworth, A. B. P. Lever, and A. A. Vlcek, *Coord. Chem. Rev.*, 1998, **174**, 469.
- <sup>17</sup> K. Krogh-Jespersen, J. D. Westbrook, J. A. Potenza and H. J. Schugar, *J. Am. Chem. Soc.*, 1987, **109**, 7025.

- 18 A. B. P. Lever, University of York, Toronto, Canada, *Private Communication*.
- 19 J. E. Ridley, M. C. Zerner, *Theor. Chim. Acta.*, 1976, **42**, 223.
- 20 E.M. Ryan, R.Wang, J.G. Vos, R.Hage, and J.G. Haasnoot, *Inorg. Chim. Acta*, 1993, **208**, 49.
- 21 B.E. Buchanan, R. Wang, J.G. Vos, R. Hage, J.G. Haasnoot, and J. Reedijk. *Inorg. Chem.*, 1990, **29**, 3263.
- 22 B.E. Buchanan, J.G. Vos, M. Kaneko, W.J.M. van der Putten, J.M. Kelly, R.Hage, R.A.G. de Graaff, R. Prins, J.G. Haasnoot, J. Reedijk, *J. Chem Soc., Dalton Trans.*, 1990, 2425.
- 23 R. Hage, J.G. Haasnoot, J. Reedijk, R. Wang, E.M. Ryan, J.G. Vos, A.L. Spek, A.J.M. Duisenberg. *Inorg. Chim. Acta*, 1990, **174**, 77.
- 24 R. Hage, J. G. Haasnoot, H. A. Nieuwenhuis, J. Reedijk, D. J. A. De Ridder and J. G. Vos., *J. Am. Chem. Soc.*, 1990, **112**, 9245.
- 25 D.P. Rillema, D.G. Taghdiri, D.S. Jones, L.A. Worl, T.J. Meyer, H.A. Levy, and C.D. Keller, *Inorg. Chem.*, 1987, **26**, 578.
- 26 D.P. Rillema, D.S. Jones, H.A. Levy, *J. Chem. Soc., Chem. Commun.*, 1979, 849.
- 27 D.S. Eggleston, K.A. Goldsby, D.J. Hodgson, T.J. Meyer, *Inorg. Chem.*, 1985, **24**, 4573.
- 28 W. R. Browne, C. M. O'Connor, H. P. Hughes, R.Hage, O. Walter, M. Doering, J. F. Gallagher, and J. G. Vos. *J. Chem. Soc. Dalton Trans.* 2002, 1740-1746.
- 29 (a)A. Juris, V. Balzani, F. Barigelletti, S. Campagna, P. Belser, and A. von Zelewsky, *Coord. Chem. Rev.*, 1988, **84**, 85. (b) J.V. Caspar, T.J. Meyer, *J. Am. Chem. Soc.*, 1983, **105**, 5583.
- 30 The level of deuteration is determined by  $^1\text{H}$  NMR spectroscopy. For the complexes, biexponential emission from different isotopomers is not observed since 95 % deuteration results in at most 1 in  $\sim 20$  positions not being exchanged with deuterium. Hence every second molecule will have one proton not exchanged and 1 in 20 molecules having two protons not exchanged *etc.* It has been shown that the effect of one proton not being exchanged is normally relatively minor and hence a monoexponential lifetime is observed {ref 31}.
- 31 (a) T.E. Keyes, F. Weldon, E. Müller, P. Pechy, M. Grätzel and J.G. Vos. *J. Chem. Soc., Dalton Trans.*, 1995, 2705 (b) T.E. Keyes, C.M. O'Connor, U. O'Dwyer, C.C. Coates, P. Callaghan, J.J. McGarvey and J.G. Vos. *J. Phys. Chem. A*, 1999, **103**, 8915 (c) W.R Browne and J.G. Vos, *Coord. Chem. Rev.* 2001, **219**, 761.
- 32 This value has been obtained using the equation;  $k_{\text{el}} = 1/\tau_{\text{complex}} - 1/\tau_{\text{model}}$ , where  $\tau_{\text{complex}}$  is the lifetime of  $[\text{Ru}(\text{phen})_2(\text{L}2)]^+$  and  $\tau_{\text{model}}$  is the lifetime of  $[\text{Ru}(\text{phen})_2(\text{L}1)]^+$ , R.J. Forster, T.E. Keyes, J.G. Vos, *Interfacial Supramolecular Assemblies*, Wiley, Chichester, 2003, p 47.
- 33 J. G. Vos, *Polyhedron*, 1992, **11**, 2285.
- 34 J. F. Ireland, P. A. H. Wyatt, *Adv. Phys. Org. Chem.*, 1976, **12**, 131,

- 35 H.A. Nieuwenhuis, J.G. Haasnoot, R. Hage, J. Reedijk, T.L. Snoeck, D.J. Stufkens, and J.G. Vos. *Inorg. Chem.*, 1991, **30**, 48
- 36 a) S. Fanni, C. Di Pietro, S. Serroni, S. Campagna, J. G. Vos, *Inorg. Chem. Commun.*, 2000, **3**, 42. B) C. Di Pietro, S. Serroni, S. Campagna, T. Gandolfi, R. Ballardini, S. Fanni, W. R. Browne and J. G. Vos, *Inorg. Chem.* 2002, **41**, 2871.
- 37 W. R. Browne, F. Weldon, A. L. Guckian, J. G. Vos, *Coll. Czech. Chem. Commun.*, 2003, **68**, 1467
- 38 M. K. Nazeeruddin, S. M. Zakeeruddin and K. Kalyanasundaram, *J. Phys. Chem.*, 1993, **97**, 9607
- 39 M.A. Haga, *Inorg. Chim. Acta*, 1980, **45**, L183 (b) P. Rillema, R. Sahai, P. Matthews, A. K. Edwards, R. J. Shaver, L. Morgan; *Inorg. Chem.*, 1990, **29**, 167. (c) M. A. Haga, M. M. Ali, S. Koseki, K. Fujimoto, A. Yoshimura, K. Nozaki, T. Ohno, K. Nakajima, D. J. Stufkens; *Inorg. Chem.*, 1996, **35**, 3335. (d) T. Ohno, K. Nozaki, M. A. Haga; *Inorg. Chem.*, 1992, **31**, 4256.
- 40 R. Hage, R. Prins, J.G. Haasnoot, J. Reedijk, and J.G. Vos. *J. Chem. Soc., Dalton Trans.*, 1987, 1389
- 41 G. E. Cabaniss, A. A. Diamantis, W. Rorer Murphy, Jr. R. W. Linton, T. J. Meyer; *J. Am. Chem. Soc.*; 1985; **107**; 1845.
- 42 A.D. Shukla, B. Whittle, H.C. Bajaj, A. Das, and M.D. Ward, *Inorg. Chim. Acta*, 1999, **285**, 89.
- 43 H. Rensmo, S. Lunell, H. Siegbahn, *J. Photochem. Photobio. A.*, 1998, **114**, 117.